ELSEVIER

Polymer 42 (2001) 7727–7738

polymer

www.elsevier.nl/locate/polymer

Investigation of free radical polymerization using diperoxyesters as bifunctional initiators

M. Benbachir*, D. Benjelloun

Laboratoire de Chimie Physique, Faculté des Sciences Dhar Mehraz, Depart. de Chimie, B.P. 1796-Atlas-Fès, Fes, Morocco

Received 13 November 2000; received in revised form 20 February 2001; accepted 16 March 2001

Abstract

An experimental investigation and a detailed kinetic model of the bulk free radical polymerization of styrene initiated by diperoxyester initiators are presented. The experiments were conducted through the full conversion range at various temperatures and initiator concentrations. It is shown that the employing of such initiators leads to the formation of polymers having substantially higher molecular weight and narrower molecular weight distribution than those obtained by the conventional monofunctional initiators. The current investigation has also found that high monomer conversion and high molecular weight can be obtained simultaneously within a reduced reaction time period. Model predictions were compared with experimental data and were found to be in agreement. © 2001 Elsevier Science Ltd. All rights reserved.

Keywords: Bifunctional initiator; Diperoxyester; Free radical polymerization

1. Introduction

In the quest for new efficient free radical initiators, we have investigated polymerization reactions using bifunctional diperoxyester initiators. The bifunctional initiator systems we shall consider in the present study are the initiators containing two labile functional groups having different thermal decomposition characteristics.

Such initiators exhibit a variety of properties that make them very useful in many polymerization and copolymerization applications. An important characteristic is that when these initiators are involved in free radical polymerization, they undergo a sequential decomposition, which generates initiator radicals continuously (as polymerization proceeds), and, therefore, allows a repeated initiation and reinitiation, as will be shown below.

The bifunctional initiators of different thermal decomposition characteristics have recently attracted an increased interest both theoretically and experimentally. The theoretical analysis accomplished by O'Driscoll and Bevington [1], has demonstrated that the sequential decomposition of two labile groups in a bifunctional initiator can affect the molecular weight distribution.

The practical advantages of using such bifunctional initiators in the polymer industry are for instance, the production of polymers having substantially high molecular weight, narrow molecular weight distribution and high monomer conversion. Besides these advantages, the reaction time can be significantly reduced with no need for modification of reactor equipment. Similar advantages are quasi-impossible with conventional monofunctional free radical initiators, or even when mixed initiator systems are used. On the other hand, the initiators considered in this work can be used in a multitude of innovative industrial applications, for instance, the block copolymerization through sequential monomer incorporation techniques [2–4]. Future work will address these issues. Our ultimate goal is to generate a database for polymerization and copolymerization of various systems initiated by multifunctional initiators, so that future extension to solution and emulsion polymerization may be accomplished in order to provide a new opportunity to the polymer industry for improving the production and controlling the polymer properties with no need for significant reactor equipment modifications as we shall show and extensively discuss in a forthcoming publication.

The purpose of the investigation reported in this article is to present a detailed kinetic model and experimental data for the isothermal free radical bulk polymerization of styrene initiated by diperoxyesters. We demonstrate in the present contribution, that the model we develop is capable of predicting the monomer conversion, molecular weight distribution (MWD) and composition distribution of reactive

* Corresponding author. Fax: +212-55733171.
E-mail address: m.benbachir@caramail.com (M. Benbachir).

PII: S0032-3861(01)00223-3

Nomenclature

f_1, f_2	initiator efficiencies of primary radicals $R_1^{\cdot}$ and $R_2^{\cdot}$, respectively
g_t	gel effect correlation factor
I	concentration of primary diperoxyester initiator (mol l^{-1})
I_0	initial concentration of primary diperoxyester initiator (mol l^{-1})
$I_{m,f}$	concentration of fast hypothetical monofunctional initiator (mol l^{-1})
$I_{0(m,f)}$	initial concentration of fast hypothetical monofunctional initiator (mol l^{-1})
$I_{m,s}$	concentration of slow hypothetical monofunctional initiator (mol l^{-1})
$I_{0(m,s)}$	initial concentration of slow hypothetical monofunctionalinitiator (mol l^{-1})
k_{d_1}, k_{d_2}	decomposition rate constants of primary initiator I and macromolecular reinitiators respectively.
k_{fm}	rate constant of chain transfer to monomer
k_{i_1}, k_{i_2}	rate constants of initiation
k_p	propagation rate constant
k_t	rate constant of combination termination
k_{t0}	rate constant of combination termination at zero conversion
M	monomer concentration (mol l^{-1})
M_0	initial concentration of monomer (mol l^{-1})
PD	polydispersity index (X_w/X_n)
R	gas constant (cal mol^{-1} K^{-1})
R_1, R_2	concentrations of primary radical species
R_J	net rate of production of any macromolecular species J
v	volume of reaction medium (l)
x	monomer conversion
X_n	overall number-average degree of polymerization
X_w	overall weight-average degree of polymerization
$X_{n,J}$	number-average degree of polymerization of macromolecular species J
$X_{w,J}$	weight-average degree of polymerization of macromolecular species J
$X_{n,d}$	number-average degree of polymerization of dead polymer
$X_{w,d}$	weight-average degree of polymerization of dead polymer

Greek letters

ϵ	volume contraction factor
$\lambda_{J,k}$	k-th moment of macromolecular species J
μ_k	k-th moment of dead polymers M_n

macromolecular species. Two experimental methods for obtaining the data are used. The experimental results are compared to the predictions of two kinetic models, which utilize different initiator systems.

It is hoped that the investigation reported here can provide a new opportunity to polymerization reaction engineers for improving the productivity and the properties of polymers.

2. Background

In contrast to the monofunctional initiators, functional groups of different thermal stabilities in the initiators under consideration in this work can undergo a sequential decomposition. Moreover, the decomposition can be controlled by varying the polymerization conditions. Pioneering studies of free radical polymerization initiated by bifunctional initiators have been reported by Prisyazhnyuk and Ivanchev [5].

The employing of such systems in free radical polymerization of vinyl or styrenic monomers, involves a kinetic mechanism in which various types of macromolecular species, carrying undecomposed functional groups, are formed in the early stages of polymerization. These macromolecular species, upon a subsequent decomposition, will be involved again in the reaction repeatedly through reinitiation, propagation and termination [6].

In this study we used the diperoxyester of the following structure:

$$\underbrace{RCOO-OOCR'COO-OOCR}_{(I)} \tag{1}$$

where: $R = CH_3(CH_2)_6-$ and $R' = -CH_2CHCl-$.

These initiators were studied by Prisyazhnyuk and Ivanchev [5]. The homolytic decomposition of the primary initiator (I) occurs as follows:

$$I \rightarrow \underbrace{RCOO}_{R_1}{}^{\cdot} + {}^{\cdot}\underbrace{OOCR'COO-OOCR}_{R_2} \tag{2}$$

$R_1^{\cdot}$ and $R_2^{\cdot}$ represent primary radical species. The decomposition of primary radical $R_2^{\cdot}$ to biradical $^{\cdot}OOC-R'-COO^{\cdot}$ is assumed to be negligible.

It is also assumed that both the peroxide groups in the primary (original) initiator I, shown in structure Eq. (1), have the same decomposition rate constant when R' is small. However, the thermal stability of a peroxide group will change when the neighbouring group decomposes [7]. On this basis, when the primary initiator I decomposes into two radical species as shown in reaction (2), the decomposition activation energy of the peroxide group in $R_2^{\cdot}$ becomes higher than that of peroxides in the primary (original) diperoxyester I. When the primary radicals $R_2^{\cdot}$ are involved in subsequent polymerization, various types of macromolecular species carrying peroxide end groups will be formed.

Table 1
Macromolecular species

Symbols	Note
$P_n^{\cdot}$: $\cdot$– – –	Live macromolecular radical of length n
$A_n^{\cdot}$: $\cdot$– – –R_2	Live macromolecular reinitiator radical of length n (carrying undecomposed peroxide)
$B_n^{\cdot}$: $\cdot$– – – $\cdot$	Live macromolecular biradical of length n
U_n: R_2– – –R_2	Polymeric reinitiator of length n (carrying two undecomposed peroxides)
V_n: – – –R_2	Polymeric reinitiator of length n (carrying undecomposed peroxide)
M_n: – – –	Dead polymer of length n

Such macromolecular species, referred to as macromolecular reinitiators, are able to decompose and then induce a subsequent polymerization again. It should pointed out that the existence of distinct types of macromolecular reinitiators in the reaction medium can generally be regarded as an 'extension' of the lifetime of the primary initiator radicals. This effect is attributed to the sequential decomposition of the reactive functional groups carrying by the bifunctional initiator.

When a diperoxyester initiator of the type of structure Eq. (1) is used in free radical polymerization, various types of macromolecular species are identified in accordance with the type of chain end units. Six distinct macromolecular species should be considered: $P_n^{\cdot}$, $A_n^{\cdot}$, $B_n^{\cdot}$, U_n, V_n and M_n as shown in Table 1.

Note that $P_n^{\cdot}$, $A_n^{\cdot}$ and $B_n^{\cdot}$ are the live macromolecular radicals and U_n, V_n, M_n are the polymers. Those macromolecular species carrying undecomposed peroxide groups on the chain ends ($A_n^{\cdot}$, U_n, V_n) can be involved again in the chain reaction through repeated reinitiation, propagation and termination as is discussed above.

3. Experimental

Two experimental methods were used in parallel under the same operating conditions. The experiments were carried out, through the full range of conversion, in borosilicate glass ampoules of length 10 cm and outer diameter 1.7 cm. The ampoules containing pure styrene were purged by vacuum-argon cycles and then hermetically sealed and placed in a temperature-controlled water bath. In order to ensure a well defined conversion vs time plot, the ampoules were removed from the bath at appropriate intervals. Conversions were measured by gravimetry and gas chromatography.

The dilatometric experiments were also conducted, using the same experimental conditions as the experiments discussed above. The dilatometric setup included a sealed dilatometer containing pure degassed styrene and a sight glass equipped with a Vernier scale to measure the meniscus level in the dilatometer. The setup was then placed in a temperature-controlled water bath.

In both cases, the experiments were accomplished at different temperatures and initiator concentrations. The values of these two parameters for each series of experiments are indicated by their respective figures shown below. The temperatures used in the experiments were: 75, 90 and 100°C, the temperature excursions were 0.1°C. The initial concentrations of the diperoxyester used for the induction of the polymerization, were: $I_0 = (0.015,\ 0.025$ and $0.050)$ mol l^{-1} and the initial monomer concentration used throughout our experiments was: $M_0 = 8.74$ mol l^{-1}.

Weight-average and number-average molecular weights were determined using size-exclusion chromatography (SEC). A polystyrene calibration curve was used.

The reproducibility of the experiments was ensured by the replication of a run at one of the experimental design points for each type of experiment. All the replicate runs were performed for: $I_0 = 0.025$ mol l^{-1} at 75°C.

4. Kinetic modelling

Our kinetic model is based on well-known principles of free radical polymerization described in various standard polymerization textbooks and extensive papers [8–15].

Several assumptions are quite common and valid and were made in order to simplify the model to some extent: (i) no impurities are present in the reaction mixture; (ii) polymerization is homogeneous; (iii) initiator decomposition occurs by thermal methods; (iv) long polymer chains are formed; (v) radical concentrations are at steady-state (QSSA); (vi) thermal initiation of styrene is negligible under 100°C [16]; (vii) β-scission, chain transfer to initiator, decarboxylation and cyclization reactions do not occur; (viii) for styrene polymerization, the termination of growing polymer chains occurs mainly by combination mechanism.

The kinetic scheme can be described as follows:

4.1. Initiation and reinitiation

$$I \xrightarrow{2k_{d_1}} R_1^{\cdot} + R_2^{\cdot} \tag{3}$$

$$R_1^{\cdot} + M \xrightarrow{k_{i_1}} P_1^{\cdot} \tag{4}$$

$$R_2^{\cdot} + M \xrightarrow{k_{i_2}} A_1^{\cdot} \tag{5}$$

$$A_n^{\cdot} \xrightarrow{k_{d_2}} B_n^{\cdot} + R_1^{\cdot} \qquad (n \geq 1) \tag{6}$$

$$U_n \xrightarrow{2k_{d_2}} A_n^{\cdot} + R_1^{\cdot} \qquad (n \geq 2) \tag{7}$$

$$V_n \xrightarrow{k_{d_2}} P_n^{\cdot} + R_1^{\cdot} \qquad (n \geq 2) \tag{8}$$

4.2. Propagation

$$P_n^{\cdot} + M \xrightarrow{k_p} P_{n+1}^{\cdot} \qquad (n \geq 1) \tag{9}$$

$$A_n^{\cdot} + M \xrightarrow{k_p} A_{n+1}^{\cdot} \qquad (n \geq 1) \tag{10}$$

$$B_n^{\cdot} + M \xrightarrow{2k_p} B_{n+1}^{\cdot} \qquad (n \geq 1) \tag{11}$$

4.3. Chain transfer to monomer

$$P_n^{\cdot} + M \xrightarrow{k_{fm}} M_n + P_1^{\cdot} \qquad (n \geq 1) \tag{12}$$

$$A_n^{\cdot} + M \xrightarrow{k_{fm}} V_n + P_1^{\cdot} \qquad (n \geq 1) \tag{13}$$

$$B_n^{\cdot} + M \xrightarrow{2k_{fm}} P_n^{\cdot} + P_1^{\cdot} \qquad (n \geq 1) \tag{14}$$

4.4. Termination

It is assumed that the termination occurs mainly by combination, then:

$$P_n^{\cdot} + P_n^{\cdot} \xrightarrow{k_t} M_{n+m} \qquad (m, n \geq 1) \tag{15}$$

$$P_n^{\cdot} + A_n^{\cdot} \xrightarrow{k_t} V_{n+m} \qquad (m, n \geq 1) \tag{16}$$

$$P_n^{\cdot} + B_m^{\cdot} \xrightarrow{2k_t} P_{n+m}^{\cdot} \qquad (m, n \geq 1) \tag{17}$$

$$A_n^{\cdot} + A_m^{\cdot} \xrightarrow{k_t} U_{n+m} \qquad (m, n \geq 1) \tag{18}$$

$$A_n^{\cdot} + B_m^{\cdot} \xrightarrow{2k_t} A_{n+m}^{\cdot} \qquad (m, n \geq 1) \tag{19}$$

$$B_n^{\cdot} + B_m^{\cdot} \xrightarrow{4k_t} B_{n+m}^{\cdot} \qquad (m, n \geq 1) \tag{20}$$

where:

I	primary (original) diperoxyester initiator;
k_{d_1}	decomposition rate constant of the peroxide groups in the primary initiator;
k_{d_2}	decomposition rate constant of the peroxide groups in the macromolecular reinitiators. k_{d_1} and k_{d_2} are independent of n [7];
k_{i_1}, k_{i_2}	rate constants of initiation;
k_p	propagation rate constant (independent of n);
k_{fm}	rate constant of chain transfer to monomer;
k_t	rate constant of combination termination.

However, at high conversion (concentrated systems) an increase in viscosity arises, which decreases the mobility of polymer chains, and the termination reactions become diffusion-controlled, thus the termination rate constant decreases seriously. This effect is called gel effect (Trommsdorff effect), and it is not quite negligible in styrene polymerization at high conversion or concentrated systems (the onset of diffusion control begins with a viscosity of 10 centipoise). To describe this effect quantitatively (g_t), numerous attempts have been made in the literature, a survey is given in Weickert [17]. The present paper will use the following gel effect correlation [18]:

$$g_t = \frac{k_t}{k_{t0}} = \exp[-2(Bx + Cx^2 + Dx^3)] \tag{21}$$

where:

$B = 2.57 - 5.05 \times 10^{-}3T$ (K);
$C = 9.56 - 1.76 \times 10^{-}2T$ (K)
$D = -3.03 + 7.85 \times 10^{-}3T$ (K);

x	monomer conversion;
k_{t0}	termination rate constant at zero conversion.

The volume contraction is described by the following equation:

$$v = v_{x=0}(1 + \epsilon x) \tag{22}$$

and the rate of relative volume contraction by:

$$\frac{1}{v}\frac{dv}{dt} = -\left(\frac{\epsilon}{M_0 + \epsilon M}\right)\frac{dM}{dt} \tag{23a}$$

$$\frac{dx}{dt} = -\frac{1 + \epsilon x}{M_0 + \epsilon M}\frac{dM}{dt} \tag{23b}$$

$$\epsilon = \frac{v_{x=1} - v_{x=0}}{v_{x=0}} \tag{23c}$$

where:

ϵ	volume contraction factor;
M_0	initial concentration of monomer.

5. Kinetic equations

Not distinguishing between a chemical species and its concentration in the notation, the kinetic expressions resulting from the kinetic scheme proposed above are as follows.

The net rate of production (R_J) of any macromolecular species J can be calculated via the following general expression:

$$R_J = \frac{d}{vdt}(Jv) = \frac{dJ}{dt} + J\frac{dv}{vdt} \tag{24}$$

5.1. For initiator and primary radicals

$$\frac{d(Iv)}{vdt} = -2k_{d_1}I \tag{25}$$

$$\frac{d(R_1 v)}{v\,dt} = 2f_1 k_{d_1} I - k_{i_1} R_1 M + k_{d_2} f_1 (A + 2U + V) \tag{26}$$

$$\frac{d(R_2 v)}{vdt} = 2f_2 k_{d_1} I - k_{i_2} R_2 M \tag{27}$$

5.2. For growing macromolecules

$$\frac{d(P_1 v)}{vdt} = k_{i_1} R_1 M - k_p M P_1 + k_{fm} M (P - P_1 + A + 2B + 2B_1) - k_t P_1 (P + A + 2B) \tag{28}$$

$$\frac{d(P_n v)}{vdt} = k_p M (P_{n-1} - P_n) + k_{d_2} V_n + k_{fm} M (2B_n - P_n) - k_t P_n (P + A + 2B) + 2k_t \sum_{m=1}^{n-1} P_{n-m} B_m \quad (n \geq 2) \tag{29}$$

$$\frac{d(A_1 v)}{vdt} = k_{i_2} R_2 M - k_p M A_1 - k_{d_2} A_1 - k_{fm} M A_1 - k_t A_1 (P + A + 2B) \tag{30}$$

$$\frac{d(A_n v)}{vdt} = -k_{d_2} A_n + 2k_{d_2} U_n + k_p M (A_{n-1} - A_n) - k_{fm} M A_n - k_t A_n (P + A + 2B) + 2k_t \sum_{m=1}^{n-1} A_{n-m} B_m \quad (n \geq 2) \tag{31}$$

$$\frac{d(B_1 v)}{vdt} = k_{d_2} A_1 - 2k_p M B_1 - 2k_{fm} M B_1 - 2k_t B_1 (P + A + 2B) \tag{32}$$

$$\frac{d(B_n v)}{vdt} = k_{d_2} A_n + 2k_p M (B_{n-1} - B_n) - 2k_{fm} M B_n - 2k_t B_n (P + A + 2B) + 2k_t \sum_{m=1}^{n-1} B_{n-m} B_m \quad (n \geq 2) \tag{33}$$

5.3. For polymer reinitiators

$$\frac{d(U_n v)}{vdt} = -2k_{d_2} U_n + \frac{k_t}{2} \sum_{m=1}^{n-1} A_{n-m} A_m \qquad (n \geq 2) \tag{34}$$

$$\frac{d(V_n v)}{vdt} = -k_{d_2} V_n + k_{fm} M A_n + k_t \sum_{m=1}^{n-1} P_{n-m} A_m \qquad (n \geq 2) \tag{35}$$

5.4. For monomer

$$\frac{d(V_n v)}{vdt} = -k_{d_2} V_n + k_{fm} M A_n + k_t \sum_{m=1}^{n-1} P_{n-m} A_m \qquad (n \geq 2) \tag{36}$$

5.5. For dead polymers

$$\frac{d(M_n v)}{vdt} = k_{fm} M P_n + \frac{k_t}{2} \sum_{m=1}^{n-1} P_{n-m} P_m \qquad (n \geq 2) \tag{37}$$

where:

f_1, f_2 initiator efficiencies of primary radicals $R_1^{\cdot}$ and $R_2^{\cdot}$ respectively, i.e. fractions being involved in initiation (constant during the polymerization);

P,A,B,U,V total of the concentrations of the corresponding macromolecular species:

$$P = \sum_{n=1}^{\infty} P_n \tag{38a}$$

$$A = \sum_{n=1}^{\infty} A_n \tag{38b}$$

$$B = \sum_{n=1}^{\infty} B_n \tag{38c}$$

$$U = \sum_{n=2}^{\infty} U_n \tag{38d}$$

$$V = \sum_{n=2}^{\infty} V_n \tag{38e}$$

6. Computation of MWD

The method of moments gives some valuable and accurate information from a reduced set of equations and much simplifies mathematics. It is perhaps the most widely used method in the modelling of polymerization reactions. The quasi-steady state approximation (QSSA) will be applied to primary radicals and live macromolecular species in solving the moment equations.

From the three first moments of the radical and dead polymer distributions, the number average and weight average degree of polymerization and, therefore, the polydispersity index (PD) can be calculated as follows:

$$\lambda_{J,K} = \sum_{n=i}^{\infty} n^k J_n \tag{39}$$

[$i = 1$ for $J = (P, A, B)$ and $i = 2$ for $J = (U, V)$]

$$\mu_k = \sum_{n=2}^{\infty} n^k M_n \tag{40}$$

$$X_n = \frac{\sum_J \lambda_{J,1} + \mu_1}{\sum_J \lambda_{J,0} + \mu_0} \qquad \text{where } J = (P, A, B, U, V) \tag{41}$$

$$X_w = \frac{\sum_J \lambda_{J,2} + \mu_2}{\sum_J \lambda_{J,1} + \mu_1} \qquad \text{where } J = (P, A, B, U, V) \tag{42}$$

$$X_{n,J} = \frac{\lambda_{J,1}}{\lambda_{J,0}} \qquad \text{where } J = (P, A, B, U, V) \tag{43a}$$

$$X_{w,J} = \frac{\lambda_{J,2}}{\lambda_{J,1}} \qquad \text{where } J = (P, A, B, U, V) \tag{43b}$$

$$X_{n,d} = \frac{\mu_1}{\mu_0} \tag{44a}$$

$$X_{w,d} = \frac{\mu_2}{\mu_1} \tag{44b}$$

$$PD = \frac{X_w}{X_n} \tag{45}$$

where:

X_n overall number-average degree of polymerization;
X_w overall weight-average degree of polymerization;
$X_{n,J}, X_{n,d}, X_{w,J}, X_{w,d}$ number-average and weight-average degree of polymerization of corresponding macromolecules $J = (P, A, B, U, V)$ and dead polymer;
PD polydispersity;
$\lambda_{J,k}, \mu_k$ k-th moment of macromolecules J and dead polymer M_n, respectively.

7. Molecular weight moment expressions

Using the kinetic equations derived above, one can derive the molecular weight moment expressions.

7.1. Macromolecular species $P_n^{\cdot}$

$$\frac{d(\lambda_{p,0}v)}{vdt} = \frac{d(Pv)}{vdt} = k_{i_1}R_1M + k_{d_2}V + k_{fm}M(A + 4B) - k_tP(P + A) \tag{46}$$

$$\frac{d(\lambda_{p,1}v)}{vdt} = k_{i_1}R_1M + k_{d_2}\lambda_{v,1} + k_pMP + k_{fm}M(P - \lambda_{p,1} + A + 2B + 2\lambda_{B,1}) + k_t[2P\lambda_{B,1} - (P + A)\lambda_{p,1}] \tag{47}$$

$$\frac{d(\lambda_{p,2}v)}{vdt} = k_{i_1}R_1M + k_{d_2}\lambda_{V,2} + k_pM(P + 2\lambda_{p,1}) + k_{fm}M(p - \lambda_{p,2} + A + 2B + 2\lambda_{B,2}) + k_t[4\lambda_{B,1}\lambda_{P,1} + 2P\lambda_{B,2} - (P + A)\lambda_{P,2}] \tag{48}$$

7.2. Macromolecular species $A_n^{\cdot}$

$$\frac{d(\lambda_{A,0}v)}{vdt} = \frac{d(Av)}{vdt} = k_{i_2}R_2M + k_{d_2}(2U - A) - k_{fm}MA - k_tA(P + A) \tag{49}$$

$$\frac{d(\lambda_{A,1}v)}{vdt} = k_{i_2}R_2M + k_{d_2}(2\lambda_{U,1} - \lambda_{A,1}) + k_PMA - k_{fm}M\lambda_{A,1} + k_t[2A\lambda_{B,1} - (P + A)\lambda_{A,1}] \tag{50}$$

$$\frac{d(\lambda_{A,2}v)}{vdt} = k_{i_2}R_2M + k_{d_2}(2\lambda_{U,2} - \lambda_{A,2}) + k_PM(A + 2\lambda_{A,1}) - k_{fm}M\lambda_{A,2} + k_t[4\lambda_{B,1}\lambda_{A,1} + 2A\lambda_{B,2} - (P + A)\lambda_{A,2}] \tag{51}$$

7.3. Macromolecular species $B_n^{\cdot}$

$$\frac{d(\lambda_{B,0}v)}{vdt} = \frac{d(Bv)}{vdt} = k_{d_2}A - 2k_tB(P + A) - 2k_{fm}MB - 2k_tB^2 \tag{52}$$

$$\frac{d(\lambda_{B,1}v)}{vdt} = k_{d_2}\lambda_{A,1} + 2k_PMB - 2k_{fm}M\lambda_{B,1} - 2k_t(P + A)\lambda_{B,1} \quad (53)$$

$$\frac{d(\lambda_{B,2}v)}{vdt} = k_{d_2}\lambda_{A,2} + 2k_PM(B + 2\lambda_{B,1}) - 2k_{fm}M\lambda_{B,2} + k_t[4\lambda_{B,1}^2 - 2(P + A)\lambda_{B,2}] \quad (54)$$

7.4. Polymeric species U_n

$$\frac{d(\lambda_{U,0}v)}{vdt} = \frac{d(Uv)}{vdt} = -2k_{d_2}U + \frac{k_t}{2}A^2 \quad (55)$$

$$\frac{d(\lambda_{U,1}v)}{vdt} = -2k_{d_2}\lambda_{U,1} + k_t\lambda_{A,1}A6 \quad (56)$$

$$\frac{d(\lambda_{U,2}v)}{vdt} = -2k_{d_2}\lambda_{U,2} + k_t(\lambda_{A,2}A + \lambda_{A,1}^2) \quad (57)$$

7.4. Polymeric species V_n

$$\frac{d(\lambda_{V,0}v)}{vdt} = \frac{d(Vv)}{vdt} = -2k_{d_2}V + k_{fm}MA + k_tPA \quad (58)$$

$$\frac{d(\lambda_{V,1}v)}{vdt} = -k_{d_2}\lambda_{V,1} + k_{fm}M\lambda_{A,1} + k_t(\lambda_{P,1}A + \lambda_{A,1}P) \quad (59)$$

$$\frac{d(\lambda_{V,2}v)}{vdt} = -k_{d_2}\lambda_{V,2} + k_{fm}M\lambda_{A,2} + k_t(\lambda_{P,2}A + 2\lambda_{P,1}\lambda_{A,1} + \lambda_{A,2}P) \quad (60)$$

7.5. Dead polymers M_n

$$\frac{d(\mu_0v)}{vdt} = k_{fm}M(P - P_1) + \frac{k_t}{2}P^2 \quad (61)$$

$$\frac{d(\mu_1v)}{vdt} = k_{fm}M(\lambda_{P,1} - P_1) + k_tP\lambda_{P,1} \quad (62)$$

$$\frac{d(\mu_2v)}{vdt} = k_{fm}M(\lambda_{P,2} - P_1) + k_t(P\lambda_{P,2} + \lambda_{P,1}^2) \quad (63)$$

$$P = \frac{-k_tA + \sqrt{(k_tA)^2 + 4k_t[2f_1k_{d_1}I + k_{d_2}(f_1A + 2U + 2V + k_{fm}M(A + 4B))]}}{2k_t} \quad (64)$$

$$A = \frac{-(k_tP + k_{d_2} + k_{fm}M) + \sqrt{(k_tP + k_{d_2} + k_{fm}M)^2 + 8k_t(f_2k_{d_1}I + k_{d_2}U)}}{2k_t} \quad (65)$$

$$B = \frac{-k_t(P + A) + k_{fm}M + \sqrt{[k_t(P + A) + k_{fm}M)]^2 + 2k_tk_{d_2}A}}{2k_t} \quad (66)$$

Applying the quasi-steady state approximation to the reaction rates generating the primary radical species and the live macromolecular species, leads to the following algebraic expressions (zeroth moments) for P, A and B:

8. Kinetic scheme with monofunctional initiators

For the purpose of comparison the bifunctional initiators with the monofunctional ones, we shall present in the following the kinetics of bulk free radical polymerization initiated by a hypothetical conventional monofunctional initiator (I_m):

8.1. Initiation by initiator

$$I_m \xrightarrow{k_d} 2R^{\cdot} \quad (67)$$

$$R^{\cdot} + M \xrightarrow{k_i} P_1^{\cdot} \quad (68)$$

8.2. Propagation

$$P_n^{\cdot} + M \xrightarrow{k_P} P_{n+1}^{\cdot} \qquad (n \geq 1) \quad (69)$$

8.3. Chain transfer to monomer

$$P_n^{\cdot} + M \xrightarrow{k_{fm}} M_n + P_1^{\cdot} \qquad (n \geq 1) \quad (70)$$

8.4. Termination

$$P_n^{\cdot} + P_m^{\cdot} \xrightarrow{k_t} M_{m+n} \; (m, n) \geq 1 \quad (71)$$

9. Kinetic equations

$$\frac{1}{v}\frac{d(I_mv)}{dt} = -k_dI_m \quad (72)$$

Table 2
Parameters for computer simulations using diperoxyester initiator I

Parameter	Value	Source
k_{d_1}	$8.90\times10^{10}\exp(-23473/RT)$, s^{-1}	[5]
k_{d_2}	$5.59\times10^{14}\exp(-30387/RT)$, s^{-1}	[5]
$k_{i1}=k_{i2}$	$1.051\times10^{7}\exp(-7060/RT)$, $l\,mol^{-1}\,s^{-1}$	[19]
k_{fm}	$3.239\times10^{5}\exp(-11190/RT)$, $l\,mol^{-1}\,s^{-1}$	[19]
k_p	$1.051\times10^{7}\exp(-7060/RT)$, $l\,mol^{-1}\,s^{-1}$	[19]
k_t	$1.260\times10^{9}\exp(-1680/RT)$, $l\,mol^{-1}\,s^{-1}$	[19]
$f_1=f_2$	0.23	[5]
ϵ	−0.147	[20]
I_0	0.025 mol l^{-1}	
M_0	8.74 mol l^{-1}	

Table 3
Parameters for computer simulations using hypothetical monofunctional initiators $I_{m,f}$ and $I_{m,s}$

Parameter	Value
k_d	For $I_{m,f}$: $k_d=8.90\times10^{10}\exp(\times23473/RT)$, s^{-1} For $I_{m,s}$: $k_d=5.59\times10^{14}\exp(\times30387/RT)$, s^{-1}
k_i	$1.051\times10^{7}\exp(\times7060/RT)$, $l\,mol^{-1}\,s^{-1}$
k_{fm}	$3.239\times10^{5}\exp(\times11190/RT)$, $l\,mol^{-1}\,s^{-1}$
k_p	$1.051\times10^{7}\exp(\times7060/RT)$, $l\,mol^{-1}\,s^{-1}$
k_t	$1.260\times10^{9}\exp(\times1680/RT)$, $l\,mol^{-1}\,s^{-1}$
f	0.23
ϵ	$\times0.147$
$I_{0(m,\,s)}=I_{0(m,\,f)}$	0.050 mol l^{-1}
M_0	8.74 mol l^{-1}

$$\frac{1}{v}\frac{d(Rv)}{dt}=2fk_dI_m-k_iRM \tag{73}$$

$$\frac{1}{v}\frac{d(P_1v)}{dt}=k_iRM-k_PMP_1+k_{fm}M(P-P_1)-k_tPP_1 \tag{74}$$

$$\frac{1}{v}\frac{d(P_nv)}{dt}=k_PM(P_{n-1}-P_n)-k_{fm}MP-k_tPP_n$$

$$(n\geq2) \tag{75}$$

$$\frac{1}{v}\frac{d(Mv)}{dt}=-k_PMP \tag{76}$$

$$\frac{1}{v}\frac{d(M_nv)}{dt}=k_{fm}MP_n+\frac{1}{2}k_t\sum_{m=1}^{n-1}P_{n-m}P_m \qquad (n\geq2) \tag{77}$$

10. Molecular weight moment expressions

The live and dead polymer moment expressions can be derived as follows.

10.1. Live macromolecules $P_n^{\cdot}$

$$\lambda_0(=P)=\sqrt{\frac{2}{k_t}fk_dI_m} \tag{78}$$

$$\lambda_1=\frac{2fk_dI_m+(k_P+k_{fm})M\lambda_0}{k_{fm}M+k_t\lambda_0} \tag{79}$$

$$\lambda_2=\frac{2fk_dI_m+k_PM(\lambda_0+2\lambda_1)+k_{fm}M\lambda_0}{k_{fm}M+k_t\lambda_0} \tag{80}$$

$$P_1=\frac{2fk_dI_m+k_{fm}M\lambda_0}{(k_P+k_{fm})M+k_t\lambda_0} \tag{81}$$

10.2. Dead polymers M_n

$$\frac{1}{v}\frac{d(\mu_0v)}{dt}=k_{fm}M(P-P_1)+\frac{1}{2}k_tP^2 \tag{82}$$

$$\frac{1}{v}\frac{d(\mu_1v)}{dt}=k_{fm}M(\lambda_{P,1}-P_1)+k_tP\lambda_{P,1} \tag{83}$$

$$\frac{1}{v}\frac{d(\mu_2v)}{dt}=k_{fm}M(\lambda_{P,2}-P_1)+k_t(P\lambda_{P,2}+\lambda_{P,1}^2) \tag{84}$$

11. Results and discussion

Indeed, both experimental methods mentioned above were found to yield similar results, however, for sake of clarity and coherence of the results, we report herein only the dataset which is collected from the experiments carried out in the glass ampoules.

Table 2 shows the numerical values of kinetic parameters and concentrations used in the simulation of the

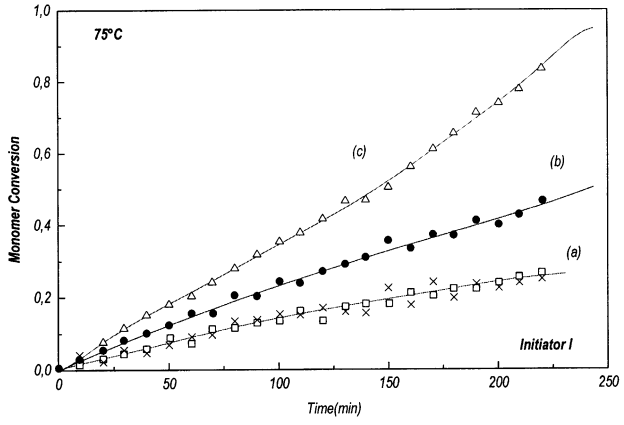

Fig. 1. Concentration effect of diperoxyesterinitiator I on monomer conversion at 75°C. (a) $I_0=0.015$ mol l^{-1}; (b) $I_0=0.025$ mol l^{-1}; (c) $I_0=0.050$ mol l^{-1}. —, Model prediction; △, □, ·, exp. data; ×, replicate run.

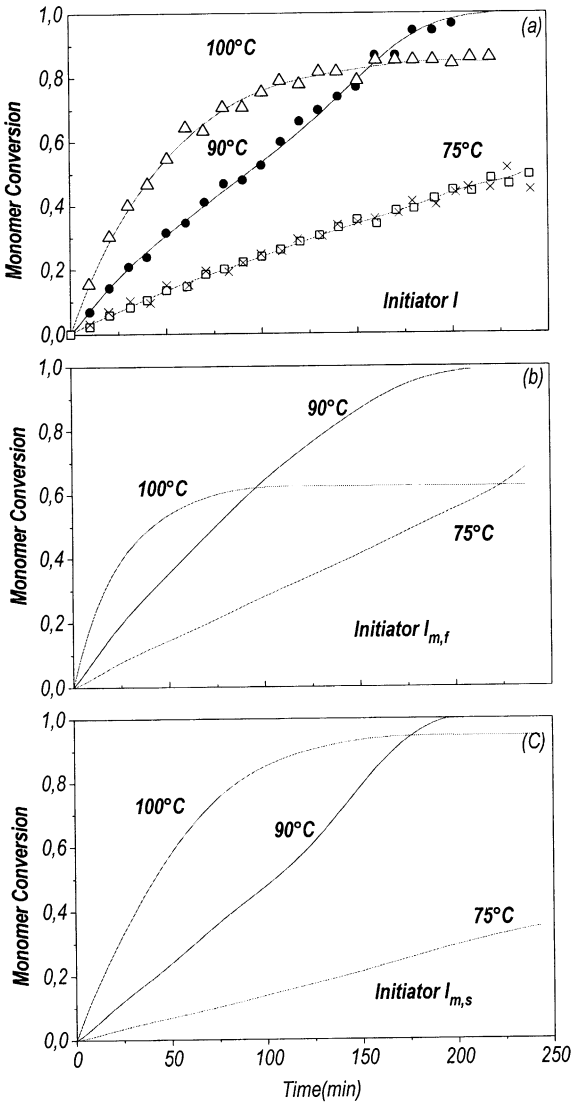

Fig. 2. Temperature effect on monomer conversion for three initiator systems. (a) $I_0 = 0.025$ mol l^{-1}; (b) $I_{0(m,f)} = 0.050$ mol l^{-1}; (c) $I_{0(m,s)} = 0.050$ mol l^{-1}. —, Model prediction; △, □, ·, exp. data; ×, replicate run.

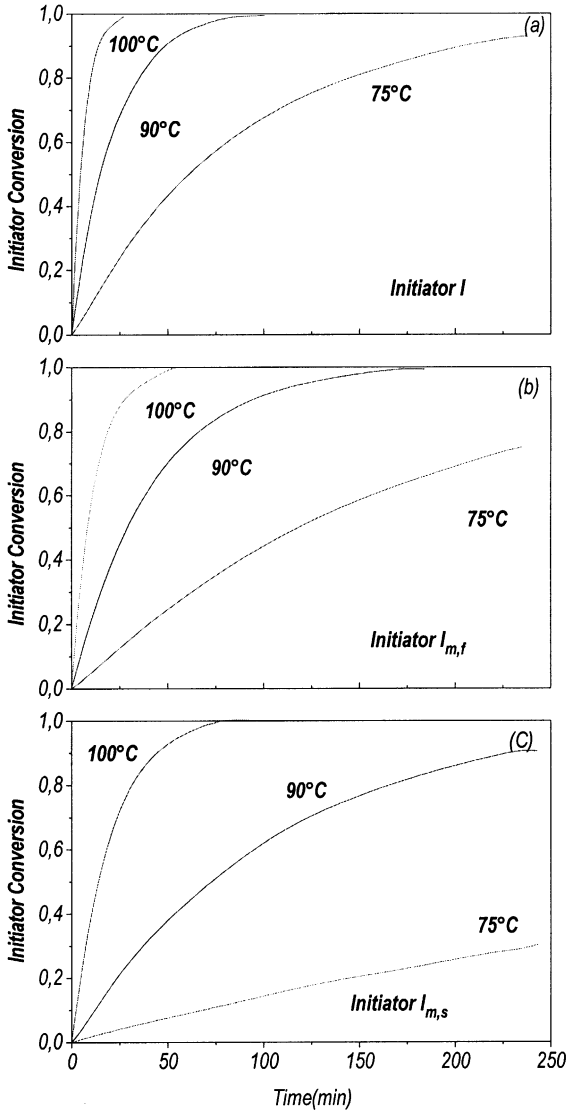

Fig. 3. Conversion profiles of three initiators at various polymerization temperatures. (a) $I_0 = 0.025$ mol l^{-1}; (b) $I_{0(m,f)} = 0.050$ mol l^{-1}; (c) $I_{0(m,s)} = 0.050$ mol l^{-1}. —, Model prediction.

polymerization initiated by the diperoxyester I which structure was shown above in the formula of Eq. (1).

Table 3 lists the values of parameters and concentrations of two hypothetical monofunctional initiators of different thermal decomposition characteristics, $I_{m,f}$ (a fast initiator, or the low temperature initiator) and $I_{m,s}$ (a slow initiator, or the high temperature initiator), used for the purpose of comparison with the bifunctional diperoxyester initiator I. Note that the relation between the equivalent concentrations of the three initiators is: $I_{0(m,s)} = I_{0(m,f)} = 2I_0$.

Computer simulations were run assuming isothermal behaviour. The modelling equations derived above were solved by the Runge–Kutta method. The two averages $\bar{M}_n$ and $\bar{M}_w$ were calculated from the SEC chromatograms. The results are presented on graphs were the solid lines represent predictions from the computer simulations and the dotted lines are the experimental results. The replicate runs were performed for: $I_0 = 0.025$ mol l^{-1} at 75°C.

The experimental data of the isothermal monomer (styrene) conversion with various concentrations of the diperoxyester I are shown in Fig. 1. The effect of initiator concentration on the monomer conversion is as expected, i.e. high initiator concentration leads to high monomer conversion.

The effect of polymerization temperature on the monomer conversion is illustrated in Fig. 2. In order to facilitate the interpretation of the effect of diperoxyester initiators, the conversion profiles of three different primary initiators (I, $I_{m,f}$, $I_{m,s}$) are shown in Fig. 3. Fig. 2(b) indicates that the dead-end polymerization phenomenon is observed about a

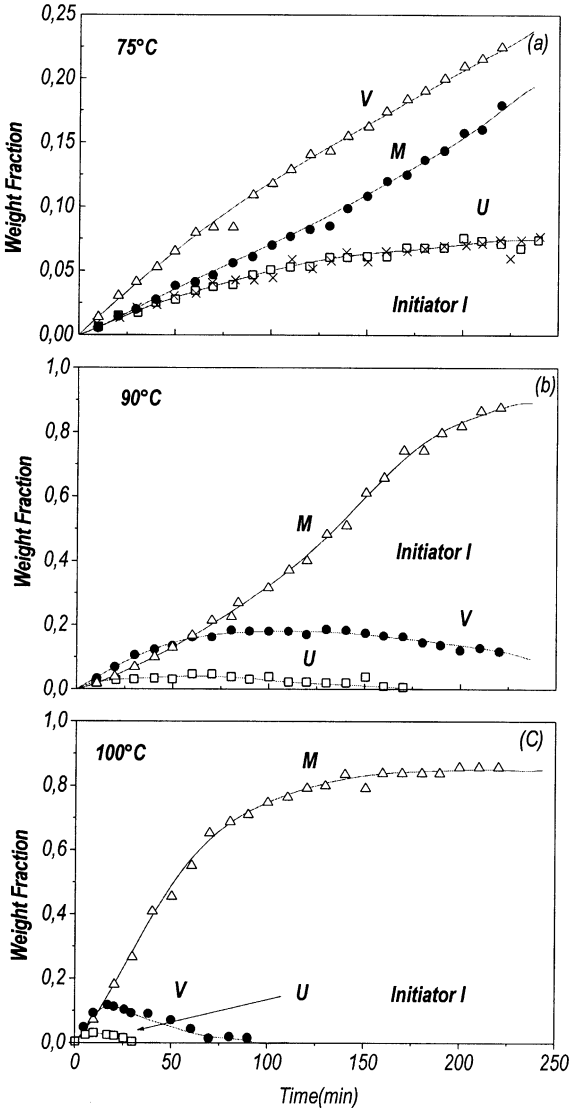

Fig. 4. Composition distribution of polymeric species (U, V, M) using diperoxyester initiator I at different temperatures. (a)–(c) $I_0 = 0.025$ mol l^{-1}. —, Model prediction; △, □, ·, exp. data; ×, replicate run.

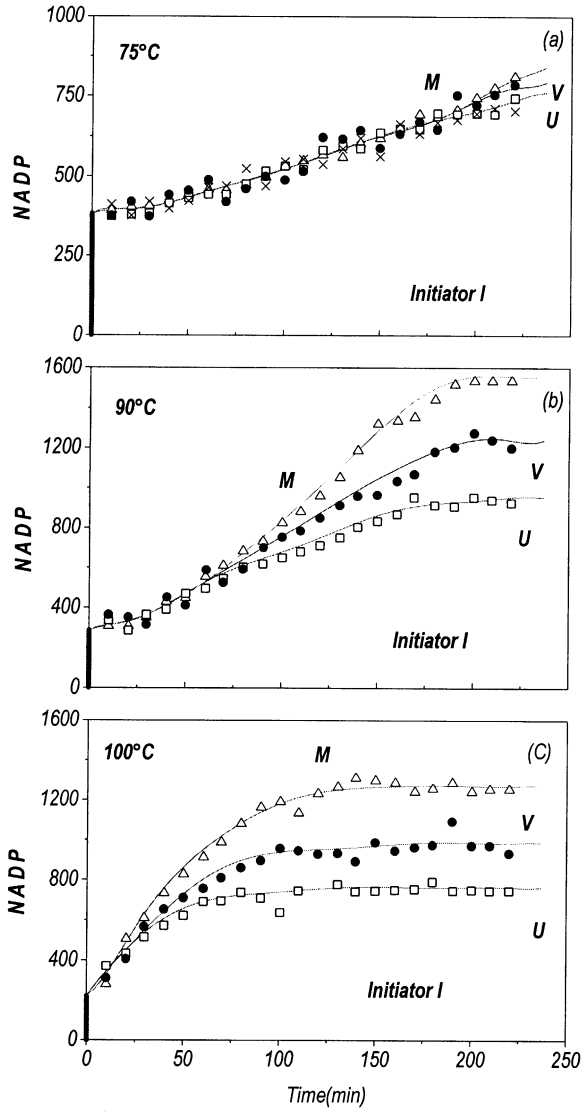

Fig. 5. Temperature effect on the NADP of polymeric species (U, V, M) using diperoxyester initiator I. (a)–(c) $I_0 = 0.025$ mol l^{-1}. —, Model prediction; △, □, ·, exp. data; ×, replicate run.

conversion of 60% at 100°C, because of the premature decomposition of the monofunctional initiator $I_{m,f}$ [Fig. 3(b)]. Whereas, when the diperoxyester initiator I is used at high temperatures [Fig. 2(a)], the monomer conversion increases continuously even if the conversion of the diperoxyester initiator is also high [Fig. 3(a)]. This behaviour is attributed to the continuous generation of the macromolecular reinitiator radicals, leading to the reinitiation, propagation and termination. Furthermore, it is seen that diperoxyester initiators, can be used for a broader range of polymerization temperatures than monofunctional ones. As is shown, the model predictions are excellent.

Fig. 4 presents the evolution of the composition distribution of polymeric reinitiators U and V, with respect to time at different temperatures when the diperoxyester initiator I is used. As high temperatures facilitate the cleavage of thermally more stable peroxide groups in these polymeric reinitiators, more reinitiator radicals are generated, and consequently, the overall monomer conversion increases even after the primary diperoxyester initiator I has been completely consumed [Fig. 3(a)].

Fig. 5 displays the overall number-average degree of polymerization (NADP) of polymeric species U, V, and M for three different polymerization temperatures. The plots indicate that much higher polymer molecular weight results during the course of polymerization. As shown, the model predictions are quite satisfactory.

Fig. 6 clearly shows that the NADP obtained by the diperoxyester initiator I, is considerably higher, particularly at high reaction temperatures. This is due to the continuous

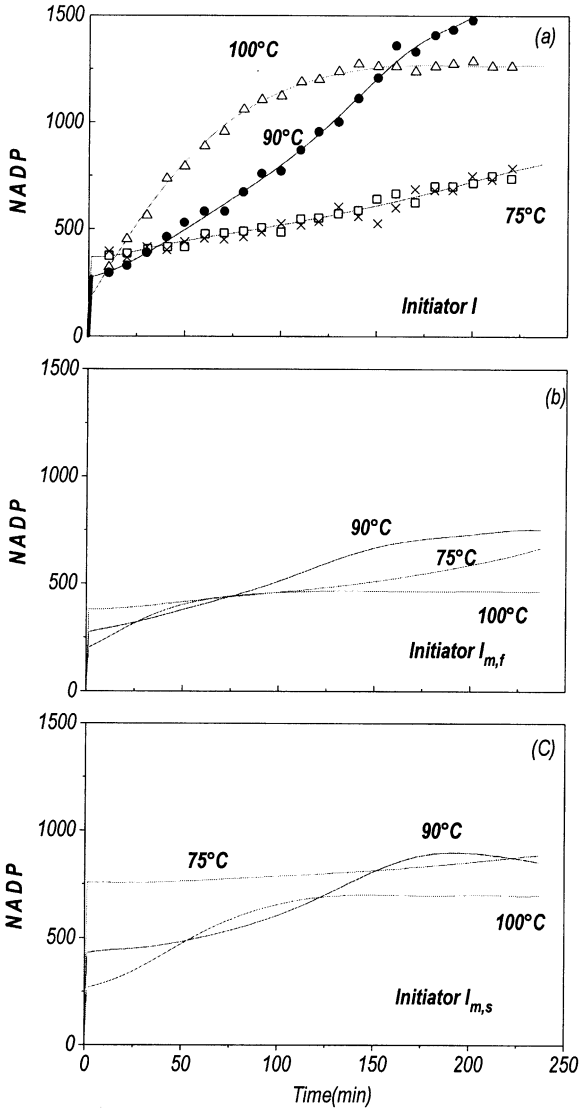

Fig. 6. Temperature effect on the NADP for three initiator systems. (a) $I_0 = 0.025$ mol l^{-1}; (b) $I_{0(m,f)} = 0.050$ mol l^{-1}; (c) $I_{0(m,s)} = 0.050$ mol l^{-1}. —, Model prediction; △, □, ·, exp. data; ×, replicate run.

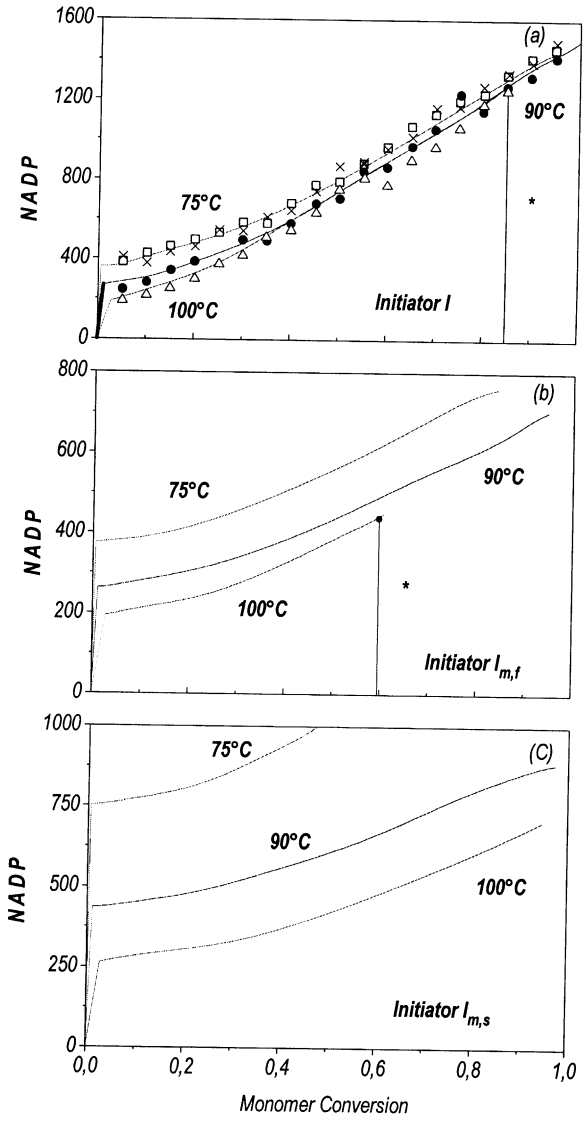

Fig. 7. Profiles of the NADP vs monomer conversion for three initiator systems at various temperatures. (a) $I_0 = 0.025$ mol l^{-1}; (b) $I_{0(m,f)} = 0.050$ mol l^{-1}; (c) $I_{0(m,s)} = 0.050$ mol l^{-1}. *, Limit of 100°C-curve; —, model prediction; △, □, ·, exp. data; ×, replicate run.

reinitiation by the macromolecular species $A_n^{\cdot}$, U_n and V_n, which contain undecomposed peroxide groups, and the termination reactions of these long macromolecular chains. Consequently, from a practical point of view, the use of such systems as diperoxyester initiator *I*, is advantageous in that batch polymerization time can be reduced substantially.

The NADP vs monomer conversion is plotted in Fig. 7 where the results show clearly that the use of diperoxyester initiators leads simultaneously to both high conversion and high molecular weight.

Finally, Fig. 8 displays the polydispersity profiles ($PD = X_w/X_n$) for three different initiators at various polymerization temperatures. As is illustrated, the bifunctional diperoxyester initiator *I* yields polymers of much narrower MWD than the fast monofunctional initiator $I_{m,f}$ even at high monomer conversion and high polymerization temperatures.

According to the results shown in Figs. 1–8, the theoretical predictions presented there are in very good agreement with the experimental data, therefore the consistency of the analysis is proved.

12. Conclusions

Of relevance to this investigation, the following conclusions can be drawn: the different thermal decomposition characteristics of the labile groups in the diperoxyester initiators lead to the formation of polymers having higher

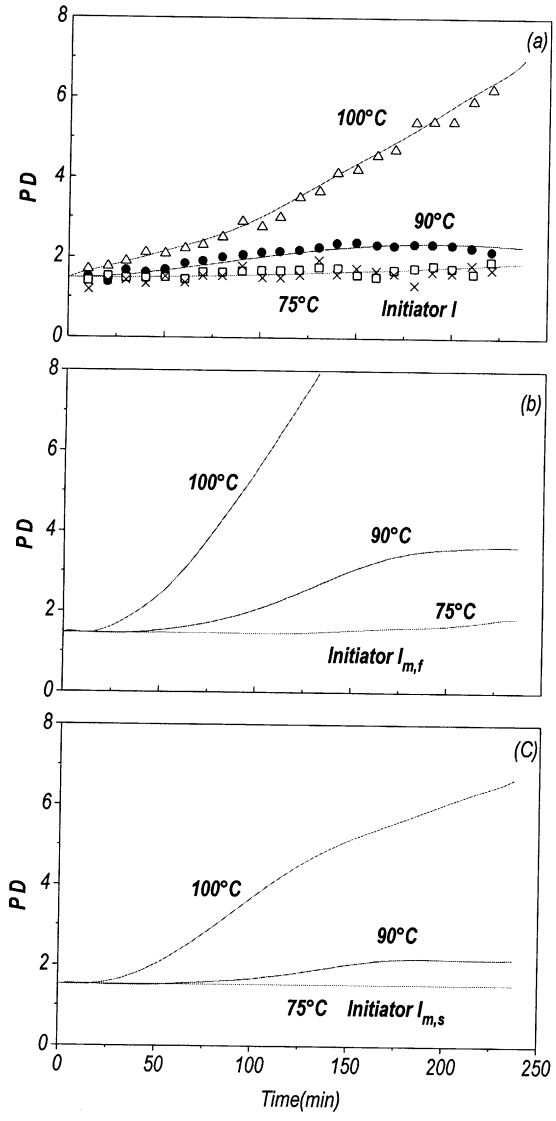

Fig. 8. Polydispersity profiles for three initiator systems at various temperatures. (a) $I_0 = 0.025$ mol l^{-1}; (b) $I_{0(m,f)} = 0.050$ mol l^{-1}; (c) $I_{0(m,s)} = 0.050$ mol l^{-1}. —, Model prediction; △, □, ·, exp. data; ×, replicate run.

molecular weight and narrower molecular weight distribution than those obtained by conventional monofunctional initiator systems. Both high monomer conversion and high molecular weight can be obtained simultaneously within a reduced reaction time period by using the diperoxyester initiators. The effect of such initiators is more pronounced at high polymerization temperatures. Model predictions are in good agreement with the experimental data. From this interplay of experimental and modelling efforts, more light is shed on the kinetic mechanism of free radical polymerization initiated by bifunctional diperoxyester initiators. The use of such initiators appears to be a promising alternative to the conventional monofunctional initiators for improving the polymer productivity and its properties more efficiently than the use of conventional monofunctional initiator systems.

Acknowledgements

The authors wish to acknowledge the support from the Computer Science Centre of Nancy (France) as well as the colleagues for their kind co-operation.

References

[1] O'Driscoll KF, Bevington JC. Eur Poly J 1985;21(12):1039.
[2] Piirma I, Chou LPHJ. Appl Poly Sci 1979;24:2051.
[3] Gunesin BZ, Piirma IJ. Appl Poly Sci 1981;26:3103.
[4] Waltz R, Heitz W. J Poly Sci Poly Chem Ed 1978;16:1807.
[5] Prisyazhnyuk AI, Ivanchev SS. Poly Sci USSR 1970;12(2):514.
[6] Kamath VR, Harpell G, U.S. Pat. 4129703, 1978.
[7] Ivanchev SS. Poly Sci USSR 1979;20:2157.
[8] Flory PJ. Principles of polymer chemistry. New York: Cornell University Press, 1953.
[9] Odian G. Principles of polymerization. 3rd ed. New York: John Wiley, 1991.
[10] Odian G, Hiraoka LSJ. Macromol Sci Chem 1972;A6:109.
[11] Villermaux J, Blavier L. Chem Engng Sci 1984;39:87.
[12] Cardenas JN, O'Driscoll KFJ. Polym Sci Polym Chem Edn 1976;14:883.
[13] Cardenas JN, O'Driscoll KFJ. Polym Sci Polym Chem Edn 1977;15:1883.
[14] Cardenas JN, O'Driscoll KFJ. Polym Sci Polym Chem Edn 1977;15:2097.
[15] Dionisio J, Mahabadi HKJ. Polym Sci Polym Chem Edn 1977;17:1891.
[16] George MH. In vinyl polymerization. New York: Dekker, 1967 p. 20.
[17] Weickert G. Mathematische modellierung der polymerisationskinetik imbereich hoher monomerumsätzeeine kritische literaturrecherche. Berlin: Plaste Kautschuk, 1986 vol. 8.
[18] Hui W, Hamielec AE. J Appl Polym Sci 1972;16:749.
[19] Brandrup J, Immergut EH. Polymer handbook. 2nd ed. New York: John Wiley, 1975.
[20] Arai K, Yamaguchi H, Saito S, Sarachina E, Yamamoto T. J Chem Engng Japan 1986;19:413.